Graphene/Hemin Hybrid Material as a Catalyst for Degradation of Alkaline Lignin with Hydrogen Peroxide

Suzhuang Yu, Li Chen, and Zongcheng Yan *

A graphene/hemin (H-GN) catalyst for lignin degradation was prepared by a wet-chemistry method with graphene oxide and hemin. Hemin was absorbed onto the graphene surface through π-π interaction. Graphene served as a supporting material for hemin, providing a large contact area between the active molecules of catalyst and substrate, as well as protecting hemin from self-oxidation and maintaining its active molecules. The H-GN catalyst showed high catalytic efficiency in the degradation of alkaline lignin under gentle conditions. At pH 13.0, the degradation rate was 49.7% with H-GN and H_2O_2 (mass ratio of H_2O_2 to lignin of 10:1) under 60 °C, which was higher than 34.9% for non-catalyst degradation. At pH 13.2, it was as high as 92.9 wt.% at 100 °C. The lignin was decomposed into small molecules with styrene as the main final product below pH 13 and with the major products of 4-hydroxy-4-methyl-2-pentanone and bis(2-ethylhexyl) phthalate at pH 13.2.

Keywords: Graphene/hemin catalyst; Wet-chemistry method; π-π-Interaction; Lignin; Degradation

*Contact information: School of Chemistry and Chemical Engineering, South China University of Technology, Guangzhou, Guangdong 510640, P.R. China; *Corresponding author: zcyan@scut.edu.cn*

INTRODUCTION

Lignin is a multifunctional phenolic polymer containing hydroxyl, carbonyl, and carboxyl groups. It is an important aromatic biopolymer composed of 30% non-fossil organic carbon (Nguyen *et al*. 2014), and it is the second most abundant naturally occurring polymer on earth. There has been extensive industrial and academic research on lignin depolymerisation, although it is difficult to degrade using either chemical or biological methods (Wu *et al.* 2005). Various methods, including thermochemical, ionic liquid, hygrogenolysis (Zhang *et al.* 2015b), photocatalysis (Li *et al.* 2015), microwave assisted technology (Dong *et al*. 2014; Ouyang *et al*. 2015a), and catalytic reduction/degradation have been explored to make lignin a value-added fuel (Zakzeski *et al*. 2010; Snowdon *et al*. 2014). Catalytic reduction/degradation methods are expected to make lignin a high-grade biofuel under gentle and environment friendly conditions (Bouxin *et al.* 2015). Additionally, catalytic processes with oxygen, hydrogen peroxide, or ozone as oxidants have been developed to degrade lignin.

Hemin, the active centre of most haemoglobin, is a natural metalloporphyrin with a simple structure (Lee *et al.* 2009). The advantages of hemin over inorganic metal catalysts include higher selectivity, lower cost, and higher surface activity (D'Souza and Muller 2007). Its activity is similar to that of the peroxidase enzyme (Guo *et al.* 2011), and it exhibits good electro catalysis based on the reversible redox of Fe(III)/Fe(II) (Kong *et al*. 2015). However, it is unstable and tends to self-oxidise, easily forming catalytic inactive dimers in oxidative media (Xue *et al.* 2012), thereby reducing catalytic activity and limiting widespread application (Zhang *et al.* 2013b). Recent research has attempted to protect the activity of hemin by modifying the

hemin construct or applying suitably biocompatible support materials (Fruk and Niemeyer 2005).

Graphene is a standard, two-dimensional, one-atom-thick sheet material consisting of sp^2-hydridised carbons (Novoselov *et al*. 2004), an extended honeycomb network, and long-range π-conjugation (Liu *et al.* 2012). Its unique construction and properties have led to its wide use in energy conversion and storage, nano-catalysts, and other applications. Combining hemin with graphene by π-π bonds is possible; graphene/hemin hybrid materials (H-GN) have high catalytic activity and maintain the special properties of both hemin and graphene (Xue *et al*. 2012; Zhang *et al*. 2012; Li *et al*. 2013).

Styrene, a bulk raw material in basic organic chemical industry, is mainly used in manufacture of polystyrene resin, ion-exchange resin, synthetic resin coatings, unsaturated polyester resin, and insulation materials. Diacetone alcohol, widely used in chemical industry, is in great demand. Bis(2-ethylhexyl) phthalate is an important general-purpose plasticizer, mainly used in PVC resin processing, polyester resin processing, acetate resin, ABS resin and rubber polymer.

An H-GN catalyst system is reusable and far less toxic than an organic solvent reaction system. It shows great potential as a green reaction system for biomass treatment. Thus, in this work, an H-GN hybrid material was synthesised via a wet-chemical method, and was investigated as an effective catalyst for lignin degradation. It was reported for the first time that styrene, diacetone alcohol and bis(2-ethyhexyl) phthalate can be converted from lignin in the presence of H-GN catalyst.

EXPERIMENTAL

Materials

Lignin (Chenming Group, Shandong, China) was recovered from soda pulping liquor by acid precipitation. Graphene oxide was purchased from Chengdu Organic Chemicals Co. Ltd. Hemin, $NaBH_4$, 30 wt.% H_2O_2 solutions were obtained from Aladdin Reagent Co., Ltd. (Shanghai, China).

Methods

Synthesis

The synthesis of H-GN hybrid materials by simple wet-chemical method (Zhang *et al*. 2013a) is shown in Fig. 1. In this process, 100 mL of a 0.5 g/L aqueous graphene oxide (GO) solution was transferred to ethanol and mixed with 100 mL of a 0.5 g/L hemin ethanol solution under ultrasonic treatment. The mixture was placed in an oil bath and heated to 65° C for 6 h after $NaBH_4$ was added.

The H-GN dispersion in ethanol was washed three times by centrifugation with ethanol to eliminate unattached hemin residue. The clean H-GN was stored in a sealed vial at room temperature. To characterise the H-GN sample, Raman spectra was carried out by LabRAM Aramis spectra (H.J.Y, France). X-ray photoelectron spectra (XPS) was determined using a ThermoFisher K-Alpha spectrophotometer (Waltham, MA, USA). UV-visible spectra was recorded on a U-3900H UV-visible spectrophotometer (Hitachi, Tokyo, Japan).

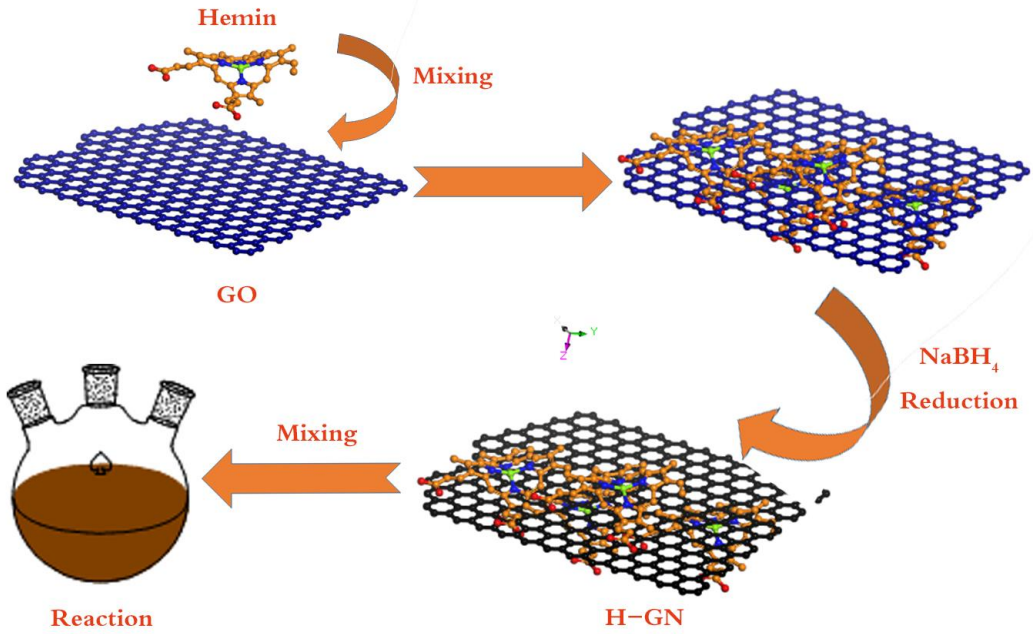

Fig. 1. H-GN hybrid material synthesis process and catalytic reaction

Degradation of alkaline lignin

A mixture containing 0.4 g of alkaline lignin, 0.01 g of H-GN catalyst, and an appropriate amount of 30 wt. % H_2O_2 was added to a 45 mL pressure seal tube. The pH of the mixture was adjusted to alkaline with 0.4 M NaOH measured by an Ohaus, starter2100 pH meter (Shanghai, China). The mixture reacted under mild conditions, and HCl was added to recover the non-degradation components, followed by centrifugal treatment and drying. The recovered H-GN catalyst was rinsed with DW, dried at 60 °C, and used to assess catalyst stability. The degradation rate (Li *et al*. 2015) was calculated according to Eq.1,

$$Degradation\ rate\ (\%) = \frac{m_0 - m_d}{m_0} \times 100 \quad (1)$$

where m_0 is the initial mass and m_d is the mass after degradation under different experimental conditions.

The products were characterised by UV/vis spectroscopy, Fourier transform infrared (FTIR) spectroscopy, gas chromatography mass spectrometry (GCMS), and high resolution mass spectrometry (HRMS). FTIR spectra were collected on a VERTEX 33 spectrophotometer (Munich, Germany) with KBr pellets. All liquid products were analysed by GCMS on a GCMS-QP2010 system (Shimadzu, Kyoto, Japan). During analysis, the column temperature was first held at 60 °C for 2 min before ramping up to 280 °C at 20 °C/min and a final hold at 280 °C for 10 min. The products were identified by the mass spectra database, and by comparing their retention times with those computer library (Ehara *et al.* 2005). HRMS spectra were detected by a maXis impact (Bruker, Germany) to further identify the degradation products.

RESULTS AND DISCUSSION

Material Characterization and Analysis

Graphene oxide (GO), hemin, and H-GN samples were characterised by Raman spectroscopy (Fig. 2). Compared with GO and hemin samples, the G and D peaks in the H-GN sample underwent a bathochromic shift to 1587 cm^{-1} (G peak) and 1328 cm^{-1} (D peak), and the ratio of I_D/I_G increased from 1.1062 to 1.2228 because of the increased small sp^2 domains and reduction average size, which indicated GN formation. Subsequently, XPS spectroscopy (Fig. 3a) exhibited N1s and Fe2p signals (Li *et al*. 2013) at 400 eV and 710 eV, respectively.

In C1s XPS spectra of GO (Fig. 3b), specific peaks were observed at 284.3, 286.4, 287.9, and 286.9 eV, corresponding to C-C, C-O, O-C=O, and C=O, respectively (Bismarck *et al.* 1997). After reduction, the intensity of the peaks corresponding to O-C=O and C=O species clearly decreased, as shown in Fig. 3c, mainly because of the removal of oxygen-containing functional groups (Zu *et al.* 2011) and double bond groups.

The N1s XPS spectra of H-GN (Fig. 3d) revealed two dominant peaks at 397.5 eV and 399.5 eV, which corresponded to C-N and Fe-N, respectively. This result confirms that most hemin molecules remain in monomer form on GN.

In the UV/Vis spectra of the H-GN dispersion after reduction (Fig. 4), the sample turned black, and the spectrogram changed, with a broad peak at 268 nm showing the formation of GN. The absorption peak at 408 nm showed that the Soret band of hemin had undergone a bathochromic shift of 9 nm, which was due to the π-π interaction between GN and hemin molecules. In sum, the results confirmed that GO was reduced to GN, and hemin was loaded on the surface of GN by the wet-chemical method.

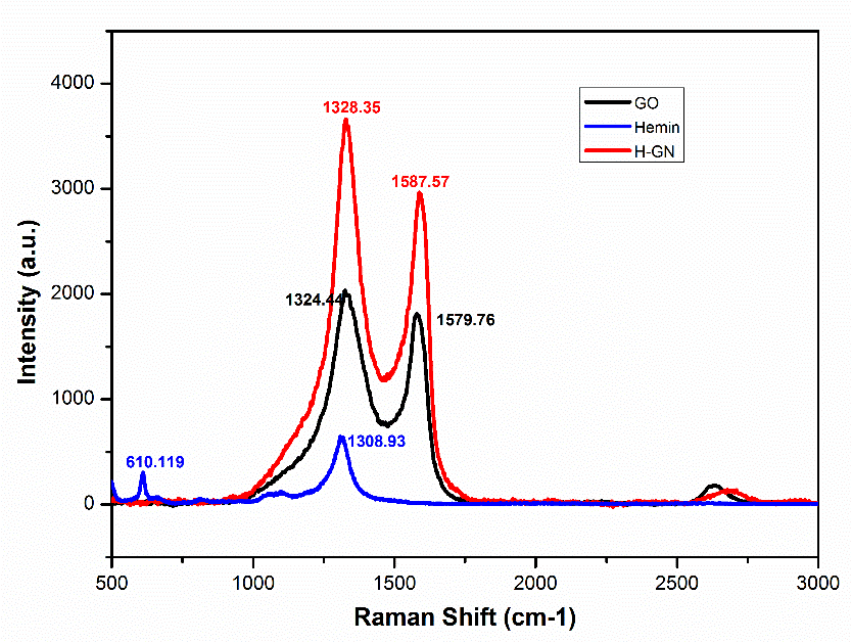

Fig. 2. Raman spectra of GO\Hemin\H-GN

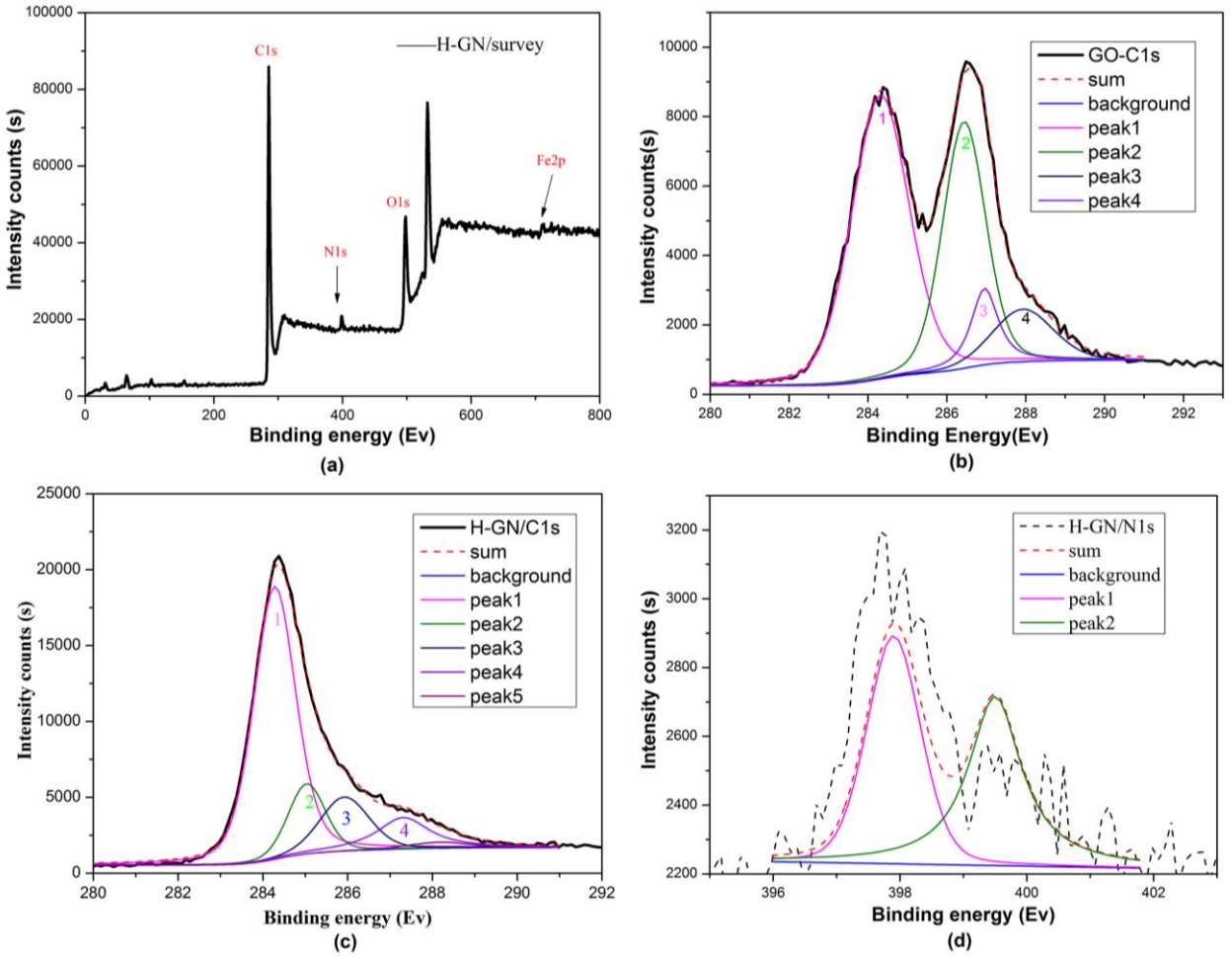

Fig. 3. XPS deconvolution of GO and H-GN. (a) Survey of H-GN; (b) deconvolution of C1s in the GO sample; (c) deconvolution of C1s in the H-GN sample; (d) deconvolution of N1s in the H-GN sample

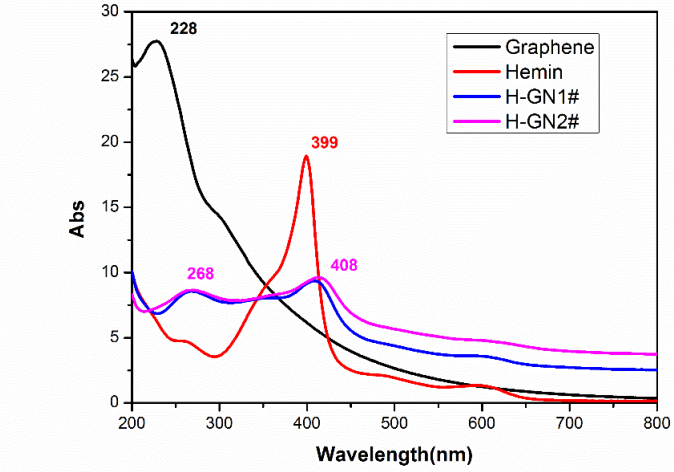

Fig. 4. UV/Vis spectra of GO\Hemin\H-GN

Catalytic Activity Result for Alkaline Lignin

Without a catalyst, the degradation rate was only 32.1% and 34.9% after a reaction time of 1 h and 5 h, respectively. Additionally, with hemin, the mixture could not react normally because of over-abundant oxygen, which caused it to bubble and overflow. Figure 5 shows the influence of reaction time and H_2O_2 dosage on lignin degradation. The degradation rate increased to 41.8% and 48.0% at 1 h and 5 h, respectively, with the addition of the H-GN catalyst. Clearly, the H-GN catalyst efficiently increased the degradation speed and degradation rate, enhancing them by 34.27%.

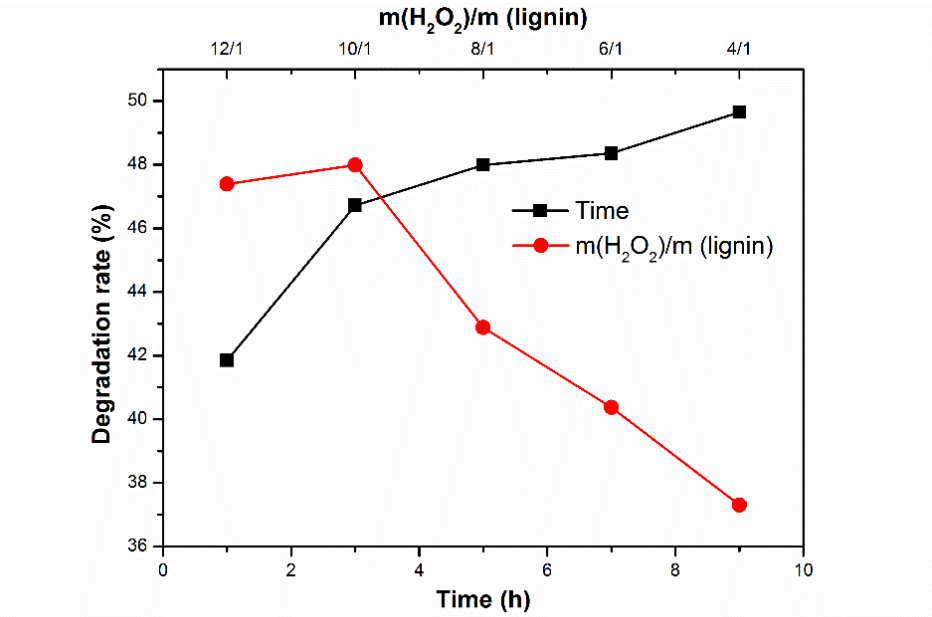

Fig. 5. Influence of reaction time and H_2O_2 dosage on lignin degradation rate. A 10:1 mass ratio of H_2O_2 to lignin and pH 13 were used when time was varied. A reaction time of 5 h and pH 13 were used when the H_2O_2-to-lignin mass ratio was varied.

Effect of 30 wt. % H_2O_2 dosage on lignin degradation

The effect of 30 wt.% hydrogen peroxide dosage on the degradation of lignin was investigated by changing the mass ratio of H_2O_2 to lignin from 4:1 to 12:1 under normal conditions at 60 °C for 5 h. Figure 5 shows that increasing H_2O_2-to-lignin ratio from 4:1 to 10:1 increased the degradation rate from 37.31 wt.% to 47.99 wt.%. Further increasing the H_2O_2-to-lignin ratio to 12:1 had little effect on degradation. As a strong oxidant, H_2O_2 produces hydroxyl radicals to form oxoiron (Fe^{4+}=O) and accelerates lignin degradation. However, excessive hydroxyl radicals formed from excess H_2O_2 may result in re-condensation of degraded lignin.

Effect of initial solution pH on lignin degradation

Figure 6 showed the effects of pH and temperature in the tested lignin solution. The effect of initial solution pH on the degradation of lignin under 60 °C for 5 h was determined. The degradation rate at pH 4, 10, 11, 12, 13, and 13.2 was 28.4%, 27.6%, 30.8%, 34.1%, 48.0%, and 73.6%, respectively. The degradation increased from 28.4% at pH 4 to 73.6% at pH 13.2, corresponding to 159% increase in activity. This observation is in agreement with the result from

Li *et al*. (2015). This effect is probably associated with the acid-base equilibrium of the adsorbed hydroxyl group; higher pH favors the generation of hydroxyl radicals. The results reveal that the H-GN catalyst is a suitable for the lignin degradation and is a new feasible way to deal with lignin degradation and reclamation.

Effect of reaction temperature on lignin degradation

The effect of reaction temperature from 40 °C to 100 °C on lignin degradation was evaluated (Fig. 6). The degradation increased with increasing temperature, and the highest lignin degradation of 92.9% was achieved at 100 °C with 0.4 M NaOH.

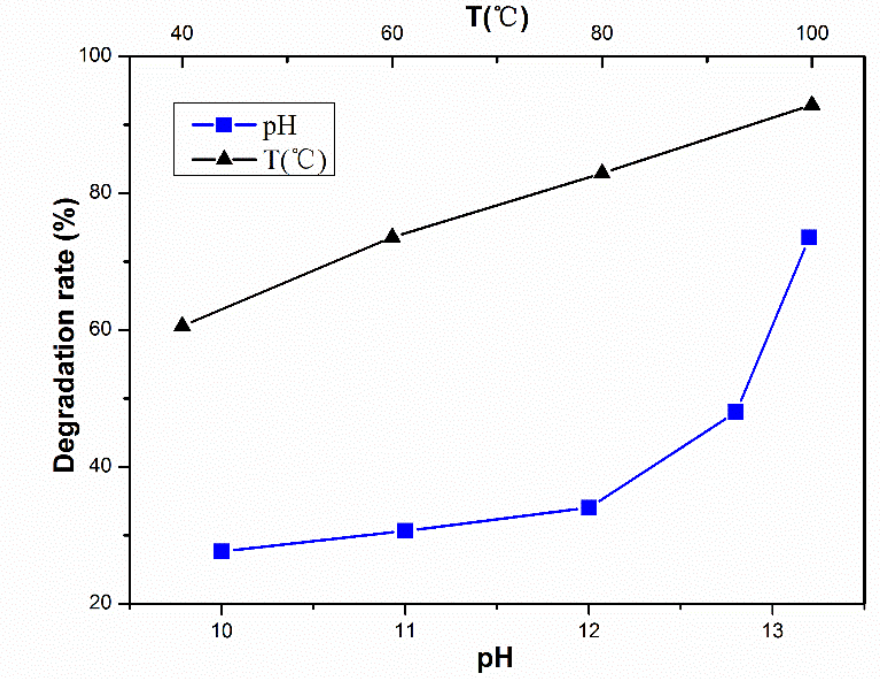

Fig. 6. Influence of pH and *T* (°C) on degradation rate of lignin. The mass ratio of H_2O_2 to lignin, time, and *T* (°C) were 10:1, 5 h, and 60 °C, respectively, when the pH was varied. The mass ratio of H_2O2 to lignin, time, and pH were 10:1, 5 h and 14 in when the *T* (°C) was varied.

Characterization of lignin before and after degradation

To further research the effects of reaction time for lignin degradation, the raw and degraded lignin were characterised by elemental analysis, UV/Vis, FTIR, GCMS, and HRMS. Elementary analysis results are shown in Fig. 7. The decrease of C and H contents and increase of O content along the degradation pattern may be explained by incorporation of oxygen from hydrogen peroxide during degradation (Wiermans *et al.* 2015).

UV/Vis spectra detected the decomposition of aromatic structures (Fig. 8). Raw lignin exhibited a strong absorbance peak at 266 nm and a shoulder peak at 280 to 286 nm, which were due to the characteristic absorbance of lignin among conjugated molecular groups, such as aromatic groups (Ouyang *et al*. 2015a). After lignin degradation by H-GN, the maximum absorbance was reduced and exhibited a hypochromatic shift of 14 nm. The hypochromatic shift reflected the reaction of the chromophoric group of lignin.

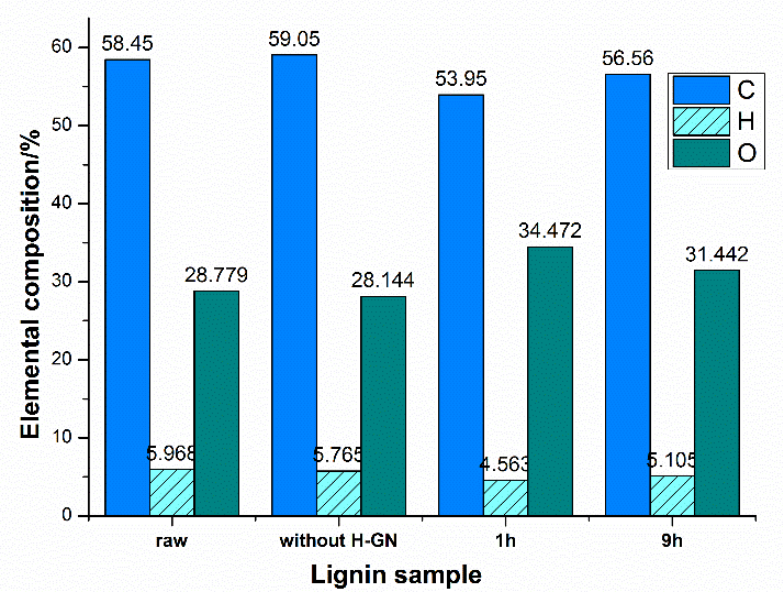

Fig. 7. Elemental analysis of raw lignin and degraded lignin

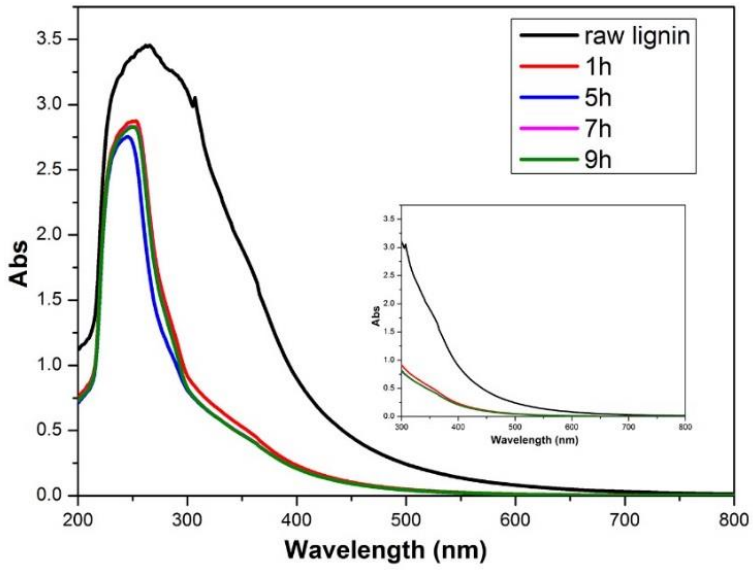

Fig. 8. UV/Vis spectra of raw lignin and degraded lignin

The FTIR spectra for raw and degraded lignin with different reaction times are shown in Fig. 9. The raw lignin curve exhibited major absorbance peaks at wavenumbers of 1600, 1365, 1144, 818, and 621 cm^{-1}, which were attributed to the absorption of aromatic nucleus vibration, aromatic nucleus stretching vibration, and C=O stretching vibration. Curve b, which represented the 1 h reaction, was similar to curve a, which showed the incomplete reaction. At increased reaction time, curves c, d, e, and f changed. Compared with raw lignin, the absorbance peaks at 1600, 1365, and 621 cm^{-1} disappeared, and the peaks at 1144 cm^{-1} and 818 cm^{-1} decreased, reflecting the opened and broken aromatic rings.

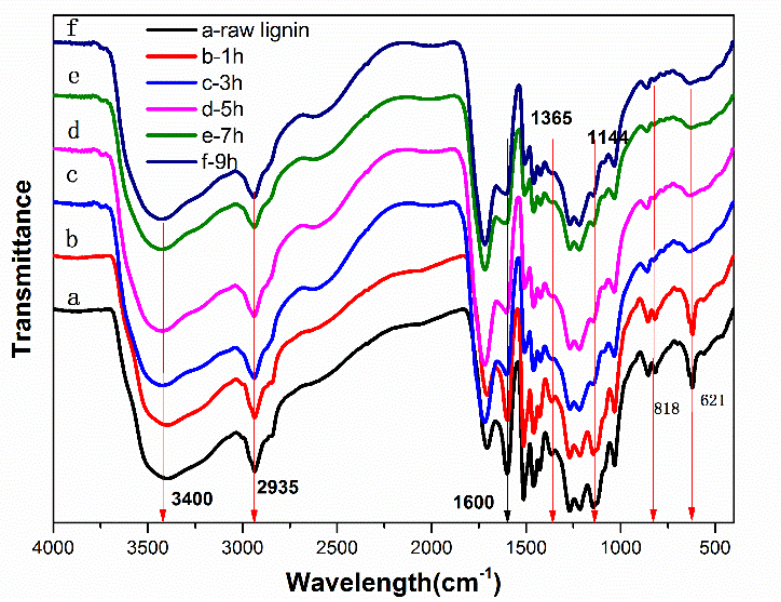

Fig. 9. FTIR spectra for raw lignin and degraded lignin with different reaction times

Liquid production from lignin degradation at different pH

GCMS analysis was used to identify the composition of degradation products (Fig. 10). Table 1 lists the major products, retention times, names, molecular formula, content, and structure detected by GCMS at an initial pH ranging from 10.0 to 13.2 for lignin degradation. Increasing the pH from 10 to 13.2 affected the products selectivity. The main product was styrene when the pH was below 13. However, the major products at pH 13.2 were 4-hydroxy-4-methyl-2-pentanone and bis(2-ethylhexyl) phthalate. HRMS analysis was carried out to further identify the products. The HRMS spectra of lignin degradation product ($C_{24}H_{38}O_4$) are shown in Fig. 11. The *m/z* ratio of the target product was 413.2662, which was the adduct mass of model compound with sodium ion. HRMS calculated for $C_{24}H_{38}O_4$ $[M+Na]^+$ 413.2662, found 413.2656. This mean that the molecular weight of the synthesized model compound was 390, which was equal to that of $C_{24}H_{38}O_4$ (Ouyang *et al.* 2015b). These may result from oxoiron (Fe^{4+}=O) species oxidizing the lignin polymer. And it was found to be highly pH-dependent (Rahikainen *et al.* 2013): an increase in pH changed the products. The higher pH value was, the more hydroxyl ions was contained. Different products of lignin degradation may be due to the cleavage of distinctive linkage.

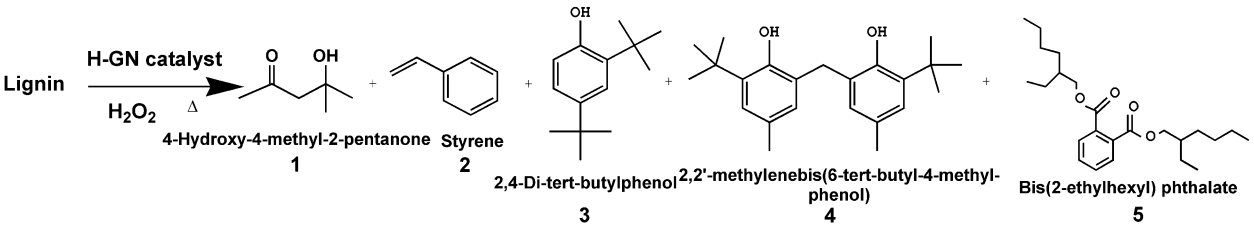

Fig. 10. Major products of lignin degradation

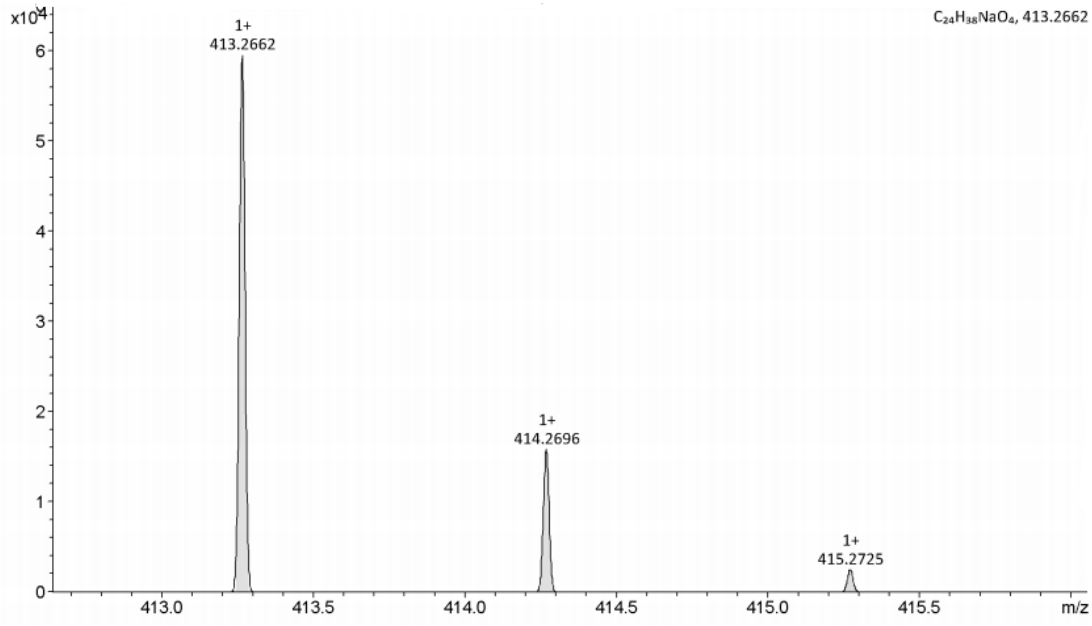

Fig. 11. HRMS spectra of lignin degradation product [bis(2-ethylhexyl) phthalate]

Table 1. GCMS of Degraded Lignin at Different pH

NO.	Retention time (min)	Products	Molecular formula	Relative area (%)				
				pH=10	pH=11	pH=12	pH=13	pH=13.2
1	3.375	4-Hydroxy-4-methyl-2-pentanone	$C_6H_{12}O_2$	6.55	5.40	4.78	——	33.82
2	4.190	Styrene	C_8H_8	73.15	39.09	90.63	82.61	——
3	10.250	2,4-Di-tert-butylphenol	$C_{14}H_{22}O$	2.02	——	——	7.20	3.21
4	15.515	2,2'-methylenebis(6-tert-butyl-4-methyl-phenol)	$C_{23}H_{32}O_2$	——	9.38	——	——	2.65
5	16.285	Bis(2-ethylhexyl) phthalate	$C_{24}H_{38}O_4$	——	——	——	——	34.95
* 13.2 was the pH value of 0.4mol/L NaOH aqueous measured by Ohaus, starter2100. * The relative percentages were calculated with peak area normalization (Zhang *et al.* 2015a).								

According to previous reports (Guo *et al.* 2011), the simplified mechanism for lignin catalytic reaction can be separated into two stages, as shown in Fig. 12. Under alkaline condition, hydrogen peroxide dissociates into hydroxyl radicals and superoxide ions that may react with hydroxyl radicals, resulting in oxygen and water as final products (Lalitendu *et al.* 2016). With the addition of the H-GN catalyst, oxygen donors from the peroxide oxidise hemin to form oxoiron (Fe^{4+}=O) (Li *et al*. 2013). Once oxoiron (Fe^{4+}=O) species accumulate to a certain level, activated Fe=O species start to weaken and break aromatic rings.

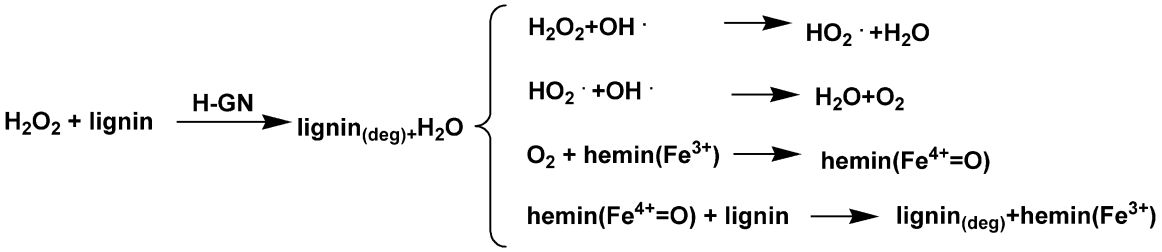

Fig. 12. Simplified mechanism for lignin catalytic reaction process

CONCLUSIONS

1. H-GN hybrid material was validated as a highly effective catalyst in lignin degradation under gentle conditions.
2. The degradation rate was as high as 92.9 wt.% at pH 13.2 with H-GN and H_2O_2, which was superior to 34.9 wt.% for non-catalyst heating degradation.
3. GCMS analysis showed that lignin was degraded into small molecules. Below pH 13, the main product was styrene; at pH 13.2, the major products were 4-hydroxy-4-methyl-2-pentanone and bis(2-ethylhexyl) phthalate.

ACKNOWLEDGEMENTS

This research was supported by National Natural Science Foundation of China (21376088). The authors also gratefully acknowledge support from the Guangdong Provincial Laboratory of Green Chemical Technology.

REFERENCES CITED

Bismarck, A., Tahhan, R., Springer, J., Schulz, A., Klapötke, T. M., Zeil, H., and Michaeli, W. (1997). "Influence of fluorination on the properties of carbon fibres," *Journal of Fluorine Chemistry* 84(2), 127-134. DOI: 10.1016/S0022-1139(97)00029-8

Bouxin, F. P., McVeigh, A., Tran, F., Westwood, N. J., Jarvis, M. C., and Jackson, S. D. (2015). "Catalytic depolymerisation of isolated lignins to fine chemicals using a Pt/alumina catalyst: Part 1-Impact of the lignin structure," *Green Chemistry* 17(2), 1235-1242. DOI: 10.1039/c4gc01678e

D'Souza, D. M., and Muller, T. J. J. (2007). "Multi-component syntheses of heterocycles by transition-metal catalysis," *Chemical Society Reviews* 36(7), 1095-1108. DOI: 10.1039/b608235c

Dong, C., Feng, C., Liu, Q., Shen, D., and Xiao, R. (2014). "Mechanism on microwave-assisted acidic solvolysis of black-liquor lignin," *Bioresource Technology* 162, 136-141. DOI: 10.1016/j.biortech.2014.03.060

Ehara, K., Takada, D., and Saka, S. (2005). "GC-MS and IR spectroscopic analyses of the lignin-

derived products from softwood and hardwood treated in supercritical water," *Journal of Wood Science* 51(3), 256-261. DOI: 10.1007/s10086-004-0653-z

Fruk, L., and Niemeyer, C. M. (2005). "Covalent hemin–DNA adducts for generating a novel class of artificial heme enzymes," *Angewandte Chemie International Edition* 44(17), 2603-2606. DOI: 10.1002/anie.200462567

Guo, Y., Li, J., and Dong, S. (2011). "Hemin functionalized graphene nanosheets-based dual biosensor platforms for hydrogen peroxide and glucose," *Sensors and Actuators B: Chemical* 160(1), 295-300. DOI: 10.1016/j.snb.2011.07.050

Kong, F.-Y., Li, W.-W., Wang, J.-Y., Fang, H.-L., Fan, D.-H., and Wang, W. (2015). "Direct electrolytic exfoliation of graphite with hemin and single-walled carbon nanotube: Creating functional hybrid nanomaterial for hydrogen peroxide detection," *Analytica Chimica Acta* 884, 37-43. DOI: 10.1016/j.aca.2015.05.016

Lalitendu, D., Praveen, K., Jason, O., Ratna, S.-S., and John, C. (2016). "Selective oxidation of lignin into aromatic aldehydes using niobium oxalate," *ASABE* 59(2). DOI: 10.13031/trans.59.10908

Lee, J., Farha, O. K., Roberts, J., Scheidt, K. A., Nguyen, S. T., and Hupp, J. T. (2009). "Metal-organic framework materials as catalysts," *Chemical Society Reviews* 38(5), 1450-1459. DOI: 10.1039/b807080f

Li, H., Lei, Z., Liu, C., Zhang, Z., and Lu, B. (2015). "Photocatalytic degradation of lignin on synthesized Ag–AgCl/ZnO nanorods under solar light and preliminary trials for methane fermentation," *Bioresource Technology* 175, 494-501. DOI: 10.1016/j.biortech.2014.10.143

Li, Y., Huang, X., Li, Y., Xu, Y., Wang, Y., Zhu, E., Duan, X., and Huang, Y. (2013). "Graphene-hemin hybrid material as effective catalyst for selective oxidation of primary C-H bond in toluene," *Scientific Reports* 1787(3), 1-7. DOI: 10.1038/srep01787

Liu, J., Qiao, Y., Guo, C. X., Lim, S., Song, H., and Li, C. M. (2012). "Graphene/carbon cloth anode for high-performance mediatorless microbial fuel cells," *Bioresource Technology* 114, 275-280. DOI: 10.1016/j.biortech.2012.02.116

Nguyen, J. D., Matsuura, B. S., and Stephenson, C. R. J. (2014). "A photochemical strategy for lignin degradation at room temperature," *Journal of the American Chemical Society* 136(4), 1218-21. DOI: 10.1021/ja4113462

Novoselov, K. S., Geim, A. K., Morozov, S. V., Jiang, D., Zhang, Y., Dubonos, S. V., Grigorieva, I. V., and Firsov, A. A. (2004). "Electric field effect in atomically thin carbon films," *Science* 306, 666-669.

Ouyang, X., Huang, X., Ruan, T., and Qiu, X. (2015a). "Microwave-assisted oxidative digestion of lignin with hydrogen peroxide for TOC and color removal," *Water Science and Technology* 71(3), 390-396. DOI: 10.2166/wst.2014.535

Ouyang, X., Yang, Y., Zhu, G., and Qiu, X. (2015b). "Radical synthesis of tetrameric lignin model compound," *Chinese Chemical Letters*, 26(8), 980-982. DOI: 10.1016/j.cclet.2015.05.011

Rahikainen, J. L., Evans, J. D., Mikander, S., Kalliola, A., Puranen, T., Tamminen, T., Marjamaa, K., and Kruus, K. (2013). "Cellulase–lignin interactions—The role of carbohydrate-binding module and pH in non-productive binding," *Enzyme and Microbial Technology*, 53(5), 315-321. DOI: 10.1016/j.enzmictec.2013.07.003

Snowdon, M. R., Mohanty, A. K., and Misra, M. (2014). "A study of carbonized lignin as an alternative to carbon black," *ACS Sustainable Chemistry & Engineering* 2(5), 1257-1263.

DOI: 10.1021/sc500086v

Wu, J., Xiao, Y.-Z., and Yu, H.-Q. (2005). "Degradation of lignin in pulp mill wastewaters by white-rot fungi on biofilm," *Bioresource Technology* 96(12), 1357-63. DOI: 10.1016/j.biortech.2004.11.019

Xue, T., Jiang, S., Qu, Y., Su, Q., Cheng, R., Dubin, S., Chiu, C.-Y., Kaner, R., Huang, Y., and Duan, X. (2012). "Graphene-supported hemin as a highly active biomimetic oxidation catalyst," *Angewandte Chemie* 124(16), 3888-3891. DOI: 10.1002/ange.201108400

Zakzeski, J., Bruijnincx, P. C. A., Jongerius, A. L., and Weckhuysen, B. M. (2010). " The catalytic valorization of lignin for the production of renewable chemicals," *Chemical Reviews* 110(6), 3552-3599. DOI: 10.1021/cr900354u

Zhang, B., Li, C., Dai, T., Huber, G. W., Wang, A., and Zhang, T. (2015a). "Microwave-assisted fast conversion of lignin model compounds and organosolv lignin over methyltrioxorhenium in ionic liquids," *RSC Advances*, 5(103), 84967-84973. DOI: 10.1039/c5ra18738a

Zhang, S., Su, L., Liu, L., and Fang, G. (2015b). "Degradation on hydrogenolysis of soda lignin using $CuO/SO_4^{2-}/ZrO_2$ as catalyst," *Industrial Crops and Products* 77, 451-457. DOI: 10.1016/j.indcrop.2015.07.039

Zhang, M., Yuan, R., Chai, Y., Chen, S., Zhong, X., Zhong, H., and Wang, C. (2012). "A cathodic electrogenerated chemiluminescence biosensor based on luminol and hemin-graphene nanosheets for cholesterol detection," *RSC Advances* 2(11), 4639. DOI: 10.1039/c2ra20374j

Zhang, Y., Xia, Z., Liu, H., Yang, M., Lin, L., and Li, Q. (2013a). "Hemin-graphene oxide-pristine carbon nanotubes complexes with intrinsic peroxidase-like activity for the detection of H2O2 and simultaneous determination for Trp, AA, DA, and UA," *Sensors and Actuators B: Chemical* 188, 496-501. DOI: 10.1016/j.snb.2013.07.010

Zhang, Y., Xu, C., and Li, B. (2013b). "Self-assembly of hemin on carbon nanotube as highly active peroxidase mimetic and its application for biosensing," *RSC Advances* 3(17), 6044-6050. DOI: 10.1039/c3ra22525a

Zu, Y., Tang, J., Zhu, W., Zhang, M., Liu, G., Liu, Y., Zhang, W., and Jia, M. (2011). "Graphite oxide-supported CaO catalysts for transesterification of soybean oil with methanol," *Bioresource Technology* 102(19), 8939-8944. DOI: 10.1016/j.biortech.2011.07.032

Article submitted: September 22, 2016; Peer review completed: December 12, 2016; Revised version received: January 12, 2017; Accepted: January 23, 2017; Published: February 10, 2017.
DOI: 10.15376/biores.12.2.2354-2366